Received: 28 January 2021 | Revised: 22 March 2021 | Accepted: 3 April 2021

DOI: 10.1002/aoc.6265

FULL PAPER

Applied Organometallic Chemistry WILEY

Synthesis, characterization, and investigation of some properties of the new symmetrical bisimine Ni(II), Zn(II), and Fe(III) complexes derived from the monoimine ligand

Eylem Dilmen Portakal[1] | **Yeliz Kaya**[1] | **Emire Demirayak**[2] | **Elif Karacan Yeldir**[3] | **Ayşe Erçağ**[1] | **İsmet Kaya**[3]

[1]Faculty of Engineering, Department of Chemistry, Inorganic Chemistry Division, Istanbul University-Cerrahpaşa, Istanbul, Turkey

[2]Department of Chemistry, Inorganic Chemistry Division, Istanbul University, Istanbul, Turkey

[3]Faculty of Sciences and Arts, Department of Chemistry, Polymer Synthesis and Analysis Lab, Çanakkale Onsekiz Mart University, Çanakkale, Turkey

Correspondence
Ayşe Erçağ, Faculty of Engineering, Department of Chemistry, Inorganic Chemistry Division, Istanbul University-Cerrahpaşa, Avcılar, Istanbul 34320, Turkey.
Email: ercaga@istanbul.edu.tr

Funding information
Scientific Research Projects Coordination Unit of Istanbul University-Cerrahpaşa, Grant/Award Number: FYL-2016-20292

The new symmetrical bisimine (ONNO donor, salen type) Ni(II), Zn(II), and Fe(III) complexes were synthesized in one step from metal ions and monoimine ligand (HL: 4-amino-3-{[(2-hydroxynaphthalen-1-yl)methylidene] amino}phenyl)(phenyl)methanone). The complexes were characterized by analytical, spectral, conductance, magnetic, and thermal data. According to these analysis results, while the bisimine ligand, spontaneously forming during complexation, is attached to the metal by two nitrogen atoms and two phenolic oxygen atoms (N_2O_2) in all complexes, in the Fe(III) complex, the fifth coordination is completed by the chlorine molecule. A square pyramidal geometry for [FeLCl] and a square planar geometry for [NiL], [ZnL] were proposed. The three-dimensional structure of [FeLC1] was also evaluated by single-crystal X-ray diffraction, and the square pyramidal structure was clearly revealed. The molar conductivity data of the complexes confirmed their nonelectrolytic nature. Poly(imine) (PL) was obtained by the oxidative polymerization reaction of HL, and some of its properties were investigated. The electrochemical properties of the ligand and the complexes were studied by means of cyclic voltammetry. Highest and lowest occupied molecular orbital (HOMO-LUMO) energy levels and electrochemical band gaps were calculated. The thermogravimetric analysis (TGA) and differential thermal analysis (DTA) of the synthesized compounds were carried out. TGA results showed that the thermal stability of the complexes is high. The solid-state electrical conductivities of the iodine doped states of the synthesized compounds were measured by the four-point probe technique. PL has approximately 35 times higher electrical conductivity than the HL and complexes. Fluorescence-sensor properties of HL were also investigated and predicted that HL could be a selective fluorescence probe for Pb^{2+}.

KEYWORDS

crystal structure, electrochemistry, fluorescence, ONNO donor bisimine complexes, TGA

1 | INTRODUCTION

Bisimines derived from 2-hydroxy-1-naphthadehyde and their metal complexes are known to have a wide range of biological activity as well as function as fluorescent chemosensors and selective electrodes.[1–7] The compounds having imine bonds (—C═N—) are known by many names such as imines, Schiff bases, azomethines, and salens. Salen- or salophen-type ligands are also called monoimines if they contain a single imine group and bisimines if they contain two imine groups. The metal bisimine complexes of four-toothed salen-type ligands, consisting of two iminonitrogens and two phenolic oxygen donors, are stable complexes due to the chelating effect and have empty axial positions for the ancillary ligand, similar to porphyrins.[8] They are used as homogeneous and heterogeneous catalyst in various organic conversion reactions.[9–11] The bisimine complexes are structurally flexible and may prefer a variety of geometries. High-performance single-molecule magnets from these type complexes have been developed.[12] These ligands and complexes continue to be of great interest due to their potential wide application.

The iron(III)–salen complexes are likely to simulate the oxygenase activity of enzymes like cytochrome P-450.[13,14] The Fe(III) complex of salen ligand derived from camphoric diamine and salicylaldehyde was evaluated as cytotoxic against melanoma, colon cancer, and breast cancer. As a result of the in vitro studies, it has been found that this complex has 20 times more curative effect than the reference chemotherapy drug.[15] In a study conducted in recent years, it has been explained that Fe(III) complexes developed from some salen derivatives show antidiabetic effect equivalent to metformin.[16] Ni(II)–salen complexes exhibit antimicrobial and DNA-binding activities and also play a key role as catalysts in the electroreductive cyclization and hydrogenation reactions.[17–20] Zn(II)-centered complexes are used to develop new materials with various photophysical, catalytic, and sensor properties.[21,22] Poly(imine)s (PLs) have nonlinear optical properties, semiconductivity, and fiber-forming ability, and some PLs also show liquid crystal properties.[23–25]

In this study, 2-hydroxy-1-naphthaldehyde instead of salicylaldehyde and 3,4-diaminobenzophenone instead of ethylene diamine were used to obtain half-unit salen-type ligand (HL), and then, tetradentate ONNO donor naphthalene complexes were obtained. Three new complexes, [FeLCI], [ZnL], and [NiL], were automatically isolated from reactions of the HL ligand with metal ions without using extra aldehyde. The synthesized compounds were characterized by a combination of elemental analysis, IR, NMR, UV–Vis, and ESI-mass spectra. Additionally, solid-state structure of [FeLCl] was determined via single-crystal X-ray diffraction. At the same time, monoimine (HL) was converted to PL by oxidative polymerization reaction using NaOCl as the oxidant. Molecular weight of PL was determined by gel permeation chromatography (GPC) technique.

The monoimine ligand (HL) used in complexation reactions was synthesized by us for the first time and presented in our previous study.[26] Its complexes and PL synthesized in this study have not been previously reported in the literature.

thermogravimetric analysis (TGA) and differential thermal analysis (DTA) were applied to determine the thermal stability of the synthesized compounds. In order to determine the semiconductor properties of the iodine doped states of these compounds, solid-state electrical conductivity was measured.

Salen-type complexes have been used as electrocatalysts.[27–30] Electrochemical studies provide valuable information regarding catalytic processes. Electrochemical properties of ligands and complexes were investigated by cyclic voltammetry (CV) to determine possible technological applications. Energy levels and electrochemical band gaps (E'_g) were calculated. The fluorescent sensor properties of HL were also investigated.

2 | EXPERIMENTAL

2.1 | Materials

3,4-Diaminobenzophenone (DAB), 2-hydroxy-1-naphthaldehyde, $NiCl_2{\cdot}6H_2O$, $ZnCl_2{\cdot}2H_2O$, $FeCl_3{\cdot}6H_2O$, acetonitrile, acetone, chloroform, dichloromethane (DCM), dimethylformamide (DMF), dimethylsulfoxide (DMSO), ethanol, methanol, ethyl acetate, hydrochloric acid, potassium hydroxide, sodium hypochlorite, and toluene were also supplied from Merck, and they were used as received.

2.2 | Physical measurements

UV–Vis spectra of the ligand and the complexes were obtained from a Shimadzu 2600 UV–Vis Spectrophotometer at 2×10^{-5} M in DMF solution. Elemental analyses were determined on a Thermo Finnigan Flash EA 1112 Series elemental analyzer. IR spectra were recorded from 4000 to 600 cm^{-1} with an Agilent Cary 630 FTIR-ATR spectrometer. ^1H NMR spectra were recorded on a Varian UNITY INOVA 500-MHz NMR spectrometer using $CDCl_3$ as solvent. The mass spectra

were recorded on a Thermo Finnigan LCQ Advantage Max LC/MS/MS spectrometer equipped with chloroform-methanol as solvent. The molar conductivities of the complexes were measured at 10^{-3} M in DMF solution at 25 ± 1°C using a digital WPA CMD 750 conductivity meter. The magnetic measurements were carried out at room temperature using the Gouy technique with an MK I model device obtained from Sherwood Scientific. Other electronic measurements were recorded at room temperature on an AnalytikJena Specord 210 spectrophotometer in DMSO. CV measurements were carried out with a CHI 660C Electrochemical Analyzer (CH Instruments, Texas, USA) at a potential scan rate of 20 mV s^{-1}. Solid-state conductivities of compounds were measured on a Keithley 2400 Electrometer. TGA-DTA measurements were performed using Perkin Elmer Diamond TGA-DTA system. Thermal properties of the ligand and their complexes were investigated in the temperature range of 20°C to 1000°C. Thermal analysis of the samples was performed in N_2 atmosphere at a heating rate of 10°C min^{-1}. Fluorescence measurements were carried out by Shimadzu RF-5301PC spectrofluorophotometer in the range 200 to 800 nm equipped with 300-W Xenon arc lamp. Slit extent of the whole of measurements was 5 nm. Malvern Viscotek GPC Dual 270 max (UK) was used for molecular weight distribution of polymer to implement the GPC measurements. The single-crystal X-ray data for [FeLCl] was collected on a Bruker D8 VENTURE diffractometer equipped with a graphite-monochromatic Mo-K_α radiation ($\lambda = 0.71073$ Å) at 304 K. The structure was solved by direct methods using the SHELXS[31] program and refined by full-matrix least-squares methods with SHELXL-2014.[32] Hydrogen atoms were refined using the riding model, and the nonhydrogen atoms were refined anisotropically. CCDC1498150 contains the supplementary crystallographic data for this article.

2.3 | Synthesis of HL

HL was synthesized by us for the first time and presented in our previous study.[26]

HL: Yield: 85%. Color: orange. Found (Calcd.) for $C_{24}H_{18}N_2O_2$ (366.41 g mol^{-1}): C, 78.14 (78.67); H, 4.41 (4.95); N, 7.25 (7.65)%. ^{1}H NMR (500 MHz, $CDCl_3$, ppm) δ: 14.75 (s, 1H, —OH), 9.42 (s, 1H, —CH═N—), 4.45 (s, 2H, —NH_2), 8.14–6.73 (aromatic protons, 14H). IR (cm^{-1}): υ(OH) 3188, υ(NH_2) 3496 and 3335, υ(C—H) 3054, υ(C═O) 1637, υ(C═N) 1601, υ(C═C) 1546, υ(C—O) 1175. UV–Vis (DMF) λ_{max} (nm): π → π* 333, n → π* 406.

2.4 | Synthesis of [FeLCl]

In 10 ml of DCM, 2 mmol of HL was dissolved. To this solution, 1 mmol of $FeCl_3 \cdot 6H_2O$ in 10 ml of ethanol was added, and the mixture was allowed to stir at room temperature for 0.5 h. The resulting red-black precipitate was filtered off and washed with cold DCM and ethanol. The product was dried with $CaCl_2$ at vacuum. The filtrate was allowed to evaporate slowly at atmospheric temperature. The dark red color crystals suitable for single-crystal X-ray diffraction analysis were obtained after about 3 weeks, washed with ethanol, and dried naturally.

[FeLCl]: Yield: 62%. m.p: 246°C to 247°C. Color: blackish red. Found (Calcd) for $C_{35}H_{22}ClFeN_2O_3$ (609.86 g mol^{-1}): C, 68.54 (68.93); H, 3.28 (3.64); N, 4.12 (4.59)%. IR (cm^{-1}): υ(C—H) 3060, υ(C═O) 1657, υ(C═N) 1615 and 1596, υ(C═C) 1533, υ(C—O) 1169. UV–Vis (DMF) λ_{max} (nm): π → π* 349, n → π* 404, LMCT 476. *m/z* (+c ESI-MS): 574.3 ($[M\text{-}Cl]^+$, 100%).

2.5 | Synthesis of [NiL] and [ZnL]

[NiL] and [ZnL] were prepared according to the method described above using $NiCl_2 \cdot 6H_2O$ and $ZnCl_2 \cdot 2H_2O$ (Scheme 1). Single crystals suitable for X-ray diffraction analysis could not be obtained.

[NiL]: Yield: 53%. m.p: >300°C. Color: red. Found (Calcd) for $C_{35}H_{22}N_2NiO_3$ (577.25 g mol^{-1}): C, 72.65 (72.82); H, 3.58 (3.84); N, 4.47 (4.85)%. ^{1}H NMR (500 MHz, $CDCl_3$, ppm) δ: 9.46 (s, 1H, —CH═N—), 8.35 (s, 1H, —CH═N—), 8.04–6.97 (aromatic protons, 20H). IR

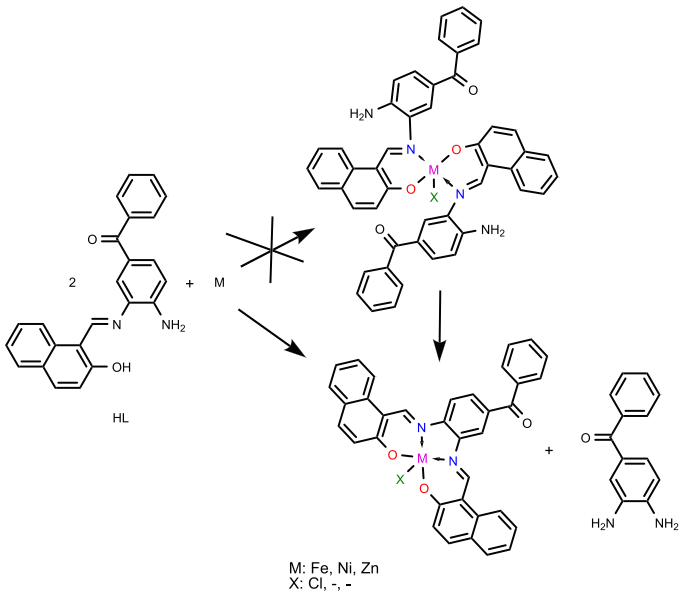

SCHEME 1 Synthesis pathway of metal complexes

(cm^{-1}): υ(C—H) 3045, υ(C═O) 1650, υ(C═N) 1601 and 1574, υ(C═C) 1529, υ(C—O) 1147. UV–Vis (DMF) λ_{max} (nm): $\pi \rightarrow \pi^*$ 333, $n \rightarrow \pi^*$ 394, LMCT 495. *m/z* (+c ESI-MS): 577.34 ($[M]^+$, 100%).

[ZnL]: Yield: 50%. m.p: >300°C. Color: red. Found (Calcd) for $C_{35}H_{22}N_2O_3Zn$ (583.97 g mol^{-1}): C, 72.45 (71.99); H, 3.54 (3.80); N, 4.31 (4.80)%. IR (cm^{-1}): υ(C—H) 3034, υ(C═O) 1648, υ(C═N) 1605 and 1575, υ(C═C) 1534, υ(C—O) 1147. UV–Vis (DMF) λ_{max} (nm): $\pi \rightarrow \pi^*$ 334, $n \rightarrow \pi^*$ 426, LMCT 479. *m/z* (+c ESI-MS): 582.8 ($[M-1]^+$, 100%).

2.6 | Synthesis of PL

HL (0.02 mol) was dissolved in two-necked round-bottom flask in THF (15 ml) and added 1 M KOH (0.5 m;). One milliliter of NaOCl was added to this mixture, and the mixture was stirred at 60°C for 24 h. At the end of 24 h, the mixture was cooled and 0.5 ml of 1 M HCl was added to the mixture. The resulting oily black product was washed with distilled water and filtered, recrystallized from ethanol, and dried in vacuum desiccators. The purity was controlled by thin-layer chromatography (TLC). The yield of PL was found as 70%. The number average molecular weight (M_n), weight average molecular weight (M_w), and polydispersity index (PDI) values of PL were found to be 8200, 8500 Da, and 1.037, respectively.

2.7 | Electrochemistry

The electrochemical properties of compounds in CH_3CN were investigated by CV studies. All the experiments were performed in a dry box filled with argon at 25°C. The system consisted of a CV cell containing glassy carbon (GCE) as the working electrode, Ag wire as the reference electrode, and platinum wire as the counter electrode. In situ spectroelectrochemical measurements were carried out by utilizing a three-electrode configuration of thin-layer quartz spectroelectrochemical cell at 25°C.

2.8 | Solid-state electrical conductivity measurements

For electrical conductivity measurements of the compounds, the powder compounds were converted to pellets using a hydraulic press developing up to 1687.2 kg cm^{-2}. Iodine doping was carried out by exposure of the pellets to iodine vapor at atmospheric pressure and room temperature in a desiccator.

2.9 | Fluorescence spectroscopy

Excitation and emission spectra of compounds film were obtained to determine the optimal emission and excitation wavelengths and Stokes shift value in deionized water. Also, the effect of transition metal ions on HL film was investigated by monitoring the fluorescence spectral behavior upon addition of several metal ions such as Cd^{2+}, Fe^{3+}, Hg^{2+}, Mn^{2+}, Ni^{2+}, Pb^{2+}, Sn^{2+}, Ag^{2+}, Cr^{2+}, and Zn^{2+} (1.0 mM) in deionized water. Concentration effect of Pb^{2+} ion on polymer film was determined using a series of metal solutions at different concentrations (in the range 1.0 to 8.0 mM) in deionized water solution. Excitation wavelength was set at 490 nm and slit width adjusted as 5 nm in the mentioned experiments.

3 | RESULT AND DISCUSSION

3.1 | Synthesis and some physical properties of the compounds

The reaction of monoimine with metal salts did not form the expected monoimine complexes. The complexes of 2-hydroxynaphthylidene symmetric bisimine were obtained without using extra aldehyde (Scheme 1). During the complexation reaction of HL with metal salts, 1 mol of HL degrades and the released aldehyde forms bisimine with the primary amine group of HL. So bisimine complexes form with the metal ions in the environment.[26] With the intramolecular modification of HL, the diamine (starting material) formed alongside the aldehyde was determined by TLC and IR in the solution in which the complex precipitated. In other words, when monoimine reacts with metal cations, it is self-rearranged and bisimine complexes form.

All complexes are colored, stable in air, and non-hygroscopic solids. The complexes are slightly soluble in solvents such as methanol, ethanol, chloroform, acetone, DMF, and DMSO. Structures of the complexes are represented in Scheme 1.

The structures of the ligand and the complexes were confirmed by elemental analysis, IR, ^1H NMR, MS, and X-ray diffraction data (for [FeLCl]).

The molar conductance values (10–14 Ω^{-1} cm^2 mol^{-1} in DMF) of Fe(III), Ni(II), and Zn(II) complexes indicate that these complexes are nonelectrolytes.[33,34]

The PL was obtained by oxidative polymerization reaction from HL.

3.2 | IR spectra

The infrared spectrum of HL clearly showed the stretching vibrations of OH, NH_2, C═N, and C═O

groups. A sharp peak observed at 1637 cm^{-1} in the ligand is assigned to C═O group stretching, which undergo minor changes in the corresponding complexes. It may therefore indicate that it is not coordinated to the metal ions. The IR spectrum of the half-unit ligand exhibits strong bands at 3496 and 3335 cm^{-1}, which is assignable to the primary amine stretches. The band at 3186 cm^{-1} is attributed to υ(OH) in IR spectrum of the half unit ligand. The phenolic υ(OH) and $\upsilon(NH_2)$ vibrations of the ligand disappeared by complexation, which indicates involvement of N and O donor atoms in coordination to the metal ions. A strong band corresponding to υ(C═N) at 1601 cm^{-1} in the free ligand shifted to lower frequencies in case of complexes, which indicates participation of the azomethine group in chelation. In addition, the strong band about 1598 cm^{-1} is assigned to second υ(C═N) in the complexes.[26,33,35,36] IR spectrums of the ligands and the complexes are given in Figures S1–S4.

3.3 | ^{1}H NMR spectra

The ^{1}H NMR spectrum of HL shows one singlet signal at 4.45 ppm for NH_2 group and one singlet signal at 14.75 ppm for OH group. These proton signals do not appear in [NiL] due to the formation of bisimine complex. The proton signal of the —CH═N— group in the monoimine ligand appears as a singlet at 9.42 ppm. Proton signals corresponding to two azomethine groups in the ^{1}H NMR spectrum of the [NiL] support the formation of the ONNO chelate structure (bisimine) (first —CH═N— group, 9.46 ppm; second —CH═N— group, 8.35 ppm). The chemical shifts of the aromatic protons appear at 8.14–6.73 ppm in the ligand and at 8.04–6.97 ppm in the [NiL]. ^{1}H NMR spectrums of HL and [NiL] are given in Figures S5 and S6. An interpretable ^{1}H NMR graphic could not be obtained for the [ZnL], probably due to its low solubility.[26,27,35,37]

3.4 | UV–Vis spectra and magnetic moments measurements

UV–Vis spectra of the ligand and the complexes were examined at 2×10^{-5} M in DMF solution. The electronic spectrum of the ligand shows a relatively intense band in the 333 nm which is assigned to a $\pi \rightarrow \pi^*$ transition and a low intensity band in the 406 nm region which is due to $n \rightarrow \pi^*$ excitation. After complex formation, these bands are monitored with the 15- to 20-nm bathochromic shifts due to extending conjugation. In addition to these bands, absorptions of the complexes have main bands in the 476–495 nm region assigned to LMCT transitions. The d-d band was not observed, as it was masked by the metal to ligand charge transfer (MLCT) band.[26,28,35]

Magnetic susceptibility measurements provide sufficient data to characterize the structure of the metal complexes. Magnetic moment measurements of complexes were carried out at room temperature (25°C). Diamagnetic nature of the Ni(II) complex was confirmed by the magnetic susceptibility measurement. This result supports square planar or distorted square planar geometry around Ni(II) ion as expected for the d^8 system. Zn(II) complex (d^{10}) is diamagnetic as expected. The magnetic moment value of the Fe(III) complex was found as 5.27 B.M.[38,39]

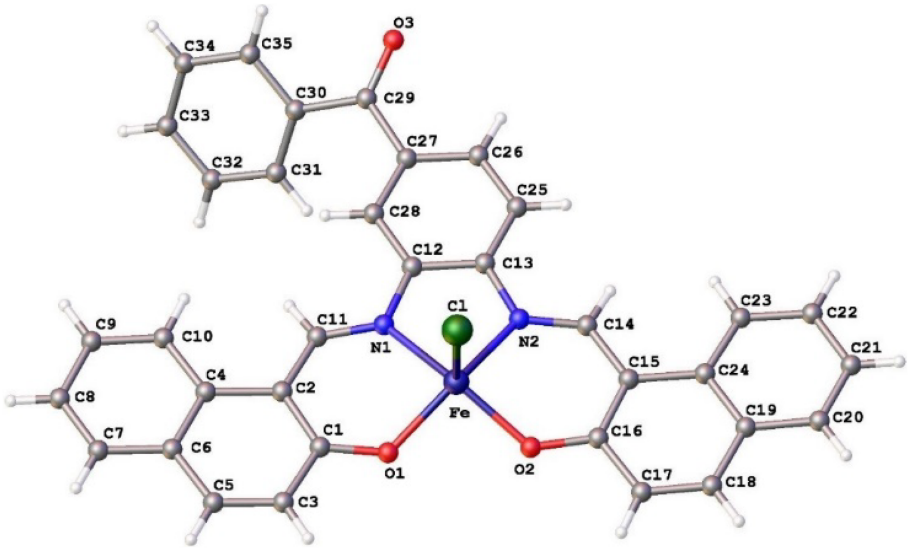

FIGURE 1 The molecular structure of [FeLCl] showing the atom numbering scheme

3.5 | Mass spectra of the metal complexes

ESI-mass spectra were obtained for all complexes. In the ESI-mass spectrum of [FeLCl], molecular ion peak with 100% relative abundance is observed at 574.3 $[M\text{-}Cl]^+$. Dechlorination is expected upon fast electron bombardment of chlorine-containing Fe(III) salen complexes. In the ESI-mass spectrum of the [NiL], molecular ion peak with 100% relative abundance was observed at 577.34 $[M]^+$. [ZnL] shows the $[M + 1]^+$ peak corresponding to molecular ion with 100% relative abundance at *m/z* 582.8. ESI-mass spectra of all the metal complexes support the proposed structures of these complexes. All mass spectrums are given in Figures S7–S9.

3.6 | X-ray crystallography

Dark red rod-like single crystals suitable for X-ray diffraction study of the [FeLCl] were obtained by the slow evaporation of mother filtrate (DCM/ethanol) at room temperature. Dark red crystal of [FeLCl], $C_{35}H_{22}ClFeN_2O_3$, having approximate dimensions of 0.010 × 0.050 × 0.400 mm was mounted on a glass fiber. The molecular structure of [FeLCl], with the atom numbering schemes, is shown in Figure 1. [FeLCl] crystallizes in a triclinic lattice with P-1 space group. The asymmetric unit of [FeLCl] contains one Fe(III) ion, one ligand, and one chlorine atom. The Fe(III) ion is coordinated by two oxygen atoms (Fe—O1 = 1.886(3) Å and Fe—O2 = 1.898(3) Å) and two nitrogen atoms (Fe—N1 = 2.086(3) Å and Fe—N2 = 2.071(3) Å) from ligand spine. The remaining fifth coordination is satisfied by a chloro ligand (Fe—Cl = 2.2199(14) Å). As a result of the fact that the Fe—O1 and Fe—O2 bonds are relatively shorter compared with Fe—N1 and Fe—N2, the five- and six-member chelate rings are not regular. Also, the bond angles of O2—Fe—N1 (147.12°) and O1—Fe—N2 (148.21°) indicate bending of square planar base in the opposite direction of chloride atom. The chlorine atom is weakly linked to the iron atom with a distance of 2.2199 Å. So the coordination geometry around the Fe(III) ions can be described as slightly distorted square pyramidal geometry, $\tau = 0.018$ (ideally $\tau = 0$).[29,40–42] There are no hydrogen bonds or significant intermolecular interactions in the crystal structure of [FeLCl]. Details of data collection and crystal structure determinations are given in Table 1. Selected bond lengths and angles of the [FeLCl] are shown in Tables S1 and S2, respectively.

TABLE 1 Crystal data and structure refinement parameters for [FeLCl]

	[FeLCl]
CCDC deposit number	1498150
Empirical formula	$C_{35}H_{22}ClFeN_2O_3$
Crystal color/shape	Dark red/rod
Formula weight	609.86
Temperature (K)	304(0)
Wavelength (Å)	0.71073
Crystal system	Triclinic
Space group	P-1
Unit cell dimensions (Å, °)	$a = 9.325(5)$ $b = 11.364(6)$ $c = 13.607(7)$ $\alpha = 84.508(15)$ $\beta = 78.868(15)$ $\gamma = 82.608(15)$
Volume (Å^3)	1399.3(13)
Cell formula units (Z)	2
Absorption coefficient (mm^{-1})	0.675
D_{calc} (g cm^{-3})	1.294
$F(000)$	626
Crystal size (mm)	0.010 × 0.050 × 0.400
θ range for data collection (°)	2.24 to 25.00
Index ranges	$-11 \le h \le 11$ $-13 \le k \le 13$ $-16 \le l \le 16$
Reflections collected	31,980
Independent reflections	4924
Coverage of independent reflections (%)	99.9
Data/parameters	4924/379
Final R indices ($I \ge 2\sigma(I)$)	$R1 = 0.0563$ $wR2 = 0.1097$
R indices (all data)	$R1 = 0.1260$ $wR2 = 0.1310$
Goodness-of-fit on F^2	1.019
Largest difference in peak and hole (e Å^{-3})	0.349/−0.335

3.7 | Thermal analysis

The thermal properties of the synthesized compounds were examined by TGA-DTA. The TGA-DTA results are listed in Table 2 and show good agreement with the formula suggested from the analytical data. The TGA and derivative thermogravimetric (DTG) curves of the HL, PL, [NiL], [ZnL], and [FeLCl] were shown in Figures 2

TABLE 2 Thermal characteristics data of HL, PL, and metal complexes

Compounds		HL	PL	[ZnL]	[NiL]	[FeLCl]
The first step	T_{on}[a]	224	190	132	454	374
	$T_{max.}$[b]	252	232	385	481	388
	T_{end}[c]	285	268	468	550	576
	%[d]	31.92	10.00	14.07	21.36	22.07
The second step	$T_{star.}$[e]	285	268	468	550	576
	$T_{max.}$	318	384	551	667	683
	T_{end}	446	620	800	776	831
	%[d]	36.27	39.09	17.86	29.01	27.26
The third step	$T_{star.}$	446	620	800	776	831
	$T_{max.}$	555	658	930	829	920
	T_{end}	1000	1000	1000	1000	1000
	%[d]	27.87	9.07	14.94	26.96	21.56
T_{20}[f]		255	339	568	496	542
T_{50}[g]		330	643	-	760	835
Char[h] (%)		3.18	41.78	53.05	20.69	29.11

[a]The onset temperature.
[b]Maximum weight loss temperature.
[c]Thermal degradation finished temperature.
[d]Weight loss at the steps.
[e]Thermal degradation started temperature.
[f]Twenty percent weight loss.
[g]Fifty percent weight loss.
[h]Char at 1000°C.

FIGURE 2 Thermogravimetric analysis (TGA) curves of HL, PL, and metal complexes

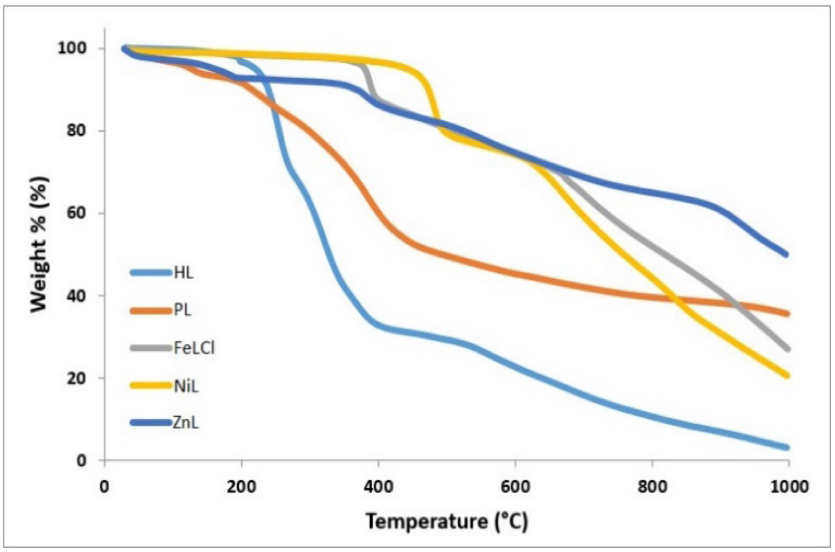

and 3. Ton temperatures of HL, PL, [FeLCl], [NiL], and [ZnL] were found to be 224°C, 190°C, 374°C, 454°C, and 132°C, respectively. Thermal degradations of all compounds were observed in three steps. In the first step, it is expected that the benzophenone group, phenyl, or CO_2 on the structures of HL, PL, [FeLCl], [NiL], and [ZnL] were separated. Also, chlorine in the structure of [FeLCl] was removed in the first step. In the second and third steps, the separation of the naphthol group or phenol groups in the structure is thought to be removed as N_2 and CO_2. As a result of the thermal analysis of HL and PL, only carbon content remains as residue, while metal complexes contain carbon and metal content as residues. The char amounts of HL, PL, [FeLCl], [NiL], and [ZnL]

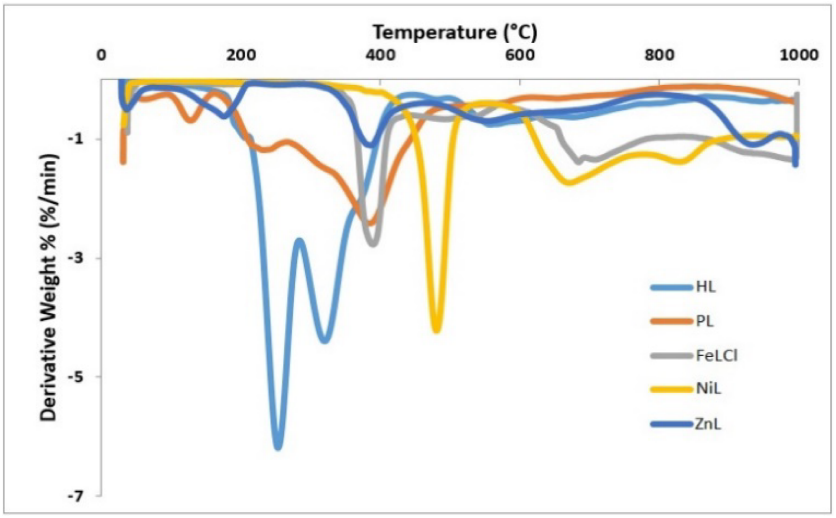

FIGURE 3 Derivative thermogravimetric (DTG) curves of HL, PL, and metal complexes

were found to be 3.18, 41.78, 29.11, 20.69, and 53.05, respectively. The char amounts of HL–Zn were higher than other compounds. According to TGA curves of [FeLCl], [NiL], and [ZnL], to be high of thermal stability of HL–metal complexes may be indicate the formation of metal–oxygen valance and metal–nitrogen coordination bond between HL–metal ions.[43] Fifty percent weight losses of HL, PL, [FeLCl], and [NiL] were found to be 330°C, 643°C, 835°C, and 760°C, respectively. The endothermic peak temperatures of HL and [FeLCl] were observed in 198°C and 363°C, respectively, at the DTA curves.

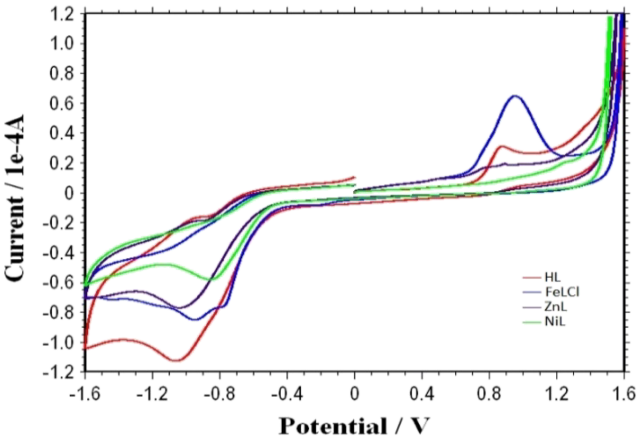

FIGURE 4 Cyclic voltammetry (CV) curves of HL and metal complexes

3.8 | Optical and electrochemical properties

Electrochemical characteristics of HL, [FeLCl], [NiL], and [ZnL] are commented by CV with a three-electrode electrochemical hall. Cyclic curves of HL, [FeLCl], [NiL], and [ZnL] are shown in Figure 4. Highest and lowest occupied molecular orbital (HOMO-LUMO) values and electrochemical band gap (E'_g) values of HL, [FeLCl], [NiL], and [ZnL] were identified in solving electronic structures of the obtained compounds. HOMO, LUMO, and E'_g values of the synthesized products were identified, as in Liu et al.[44] and Cernini et al.,[45] and the calculated results are summarized in Table 3. The lowest electrochemical band gap (E'_g) values were observed in [NiL].

The onset oxidation potential (E_{ox}) of HL, [FeLCl], [NiL], and [ZnL] are in the range of 0.8760–0.9510 V and calculated HOMO level of HL, [FeLCl], [NiL], and [ZnL] were −5.266, − 5.341, −5.279, and −5.266 eV, respectively. As similar, the onset reduction potential (E_{red}) of HL, [FeLCl], [NiL], and [ZnL] were between −0.9920 and (−1.0670) V; LUMO energy levels of these chemicals were identified as −3.323, −3.442, −3.398, and −3.361 eV, respectively. The electrochemical band gaps (E'_g) of HL, [FeLCl], [NiL], and [ZnL] were also calculated as 1.943, 1.899, 1.881, and 1.905 eV, respectively. As seen, the E'_g values of HL, [FeLCl], [NiL], and [ZnL] were very similar to each other. However, the E'_g value of [NiL] was slightly lower, and [NiL] has the low-electrochemical band gaps.

3.9 | Solid-state electrical conductivities

The electrical conductivity values of HL, PL, [FeLCl], [NiL], and [ZnL] were measured by iodine doping at room temperature. The electrical conductivity values of HL, PL, [FeLCl], [NiL], and [ZnL] were calculated to be 4.25×10^{-5}, 135×10^{-5}, 4.33×10^{-5}, 3.85×10^{-5}, and 4.10×10^{-5} S cm^{-1}, respectively. These results showed that all compounds are on the semiconductor level.

3.10 | Fluorescence spectra

The solid-state fluorescence spectra of the ligand and its complex were recorded. For the ligand, there are two emissions. Excitation and emission spectra of compounds film were obtained due to determine the optimal emission and excitation wavelengths and Stokes shift value in deionized water.

Also, transition metal ions effect on HL film was investigated by monitoring the fluorescence spectral behavior upon addition of several metal ions such as Cd^{2+}, Fe^{3+}, Hg^{2+}, Mn^{2+}, Ni^{2+}, Pb^{2+}, Sn^{2+}, Ag^{2+}, Cr^{2+}, and Zn^{2+} (1.0 mM) in deionized water. Concentration effect of Pb^{2+} ion on polymer film was determined using a series of different concentrated metal solutions (in the range 1.0 to 8.0 mM) in deionized water solution. Excitation wavelength was set at 490 nm and slit width adjusted as 5 nm in the mentioned experiments.

Fluorescence analysis of the complexes of HL with Pb^{2+}, Fe^{3+}, Zn^{2+}, Ni^{2+}, Hg^{2+}, Mn^{2+}, Sn^{2+}, and Ag^{+} metals were made, and their spectra are shown in Figure 5. When the concentration of each metal used is

TABLE 3 CV results of HL and metal complexes

Compound	E_{ox}[a] (eV)	E_{red}[b] (eV)	HOMO (eV)	LUMO (eV)	E'_g[c] (eV)
HL	0.8760	−1.0670	−5.266	−3.323	1.943
[FeLCl]	0.9510	−0.9480	−5.341	−3.442	1.899
[NiL]	0.8890	−0.9920	−5.279	−3.398	1.881
[ZnL]	0.8760	−1.0290	−5.266	−3.361	1.905

Abbreviations: CV, cyclic voltammetry; HOMO, highest occupied molecular orbital; LUMO, lowest occupied molecular orbital.
[a]Onset oxidation potential.
[b]Onset reduction potential.
[c]Electrochemical band gap.

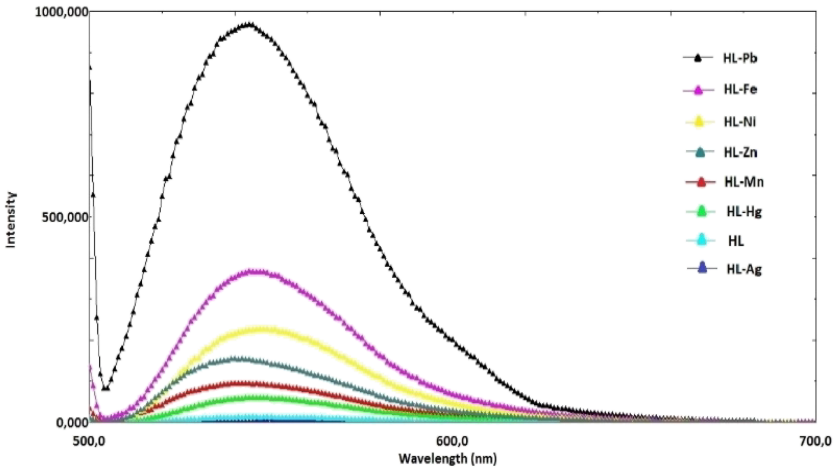

FIGURE 5 Florescence emission spectra of HL–metal complexes (slit width 5 nm, excitation wavelength 490 nm, and concentration of metals 1.00 mM)

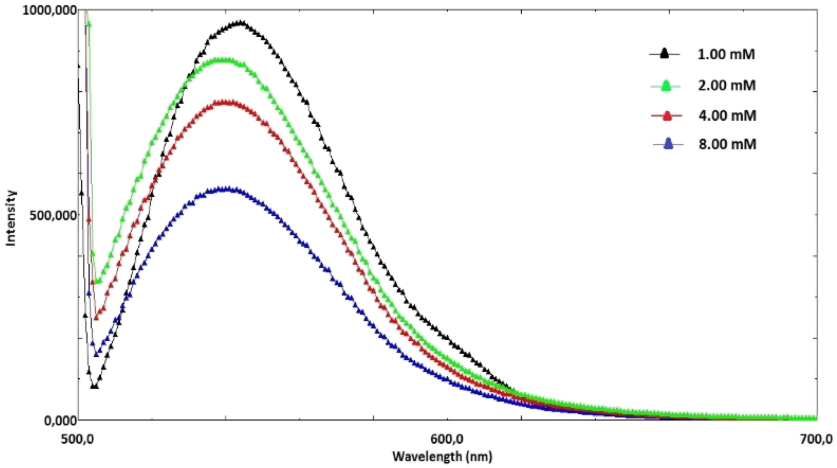

FIGURE 6 Florescence emission spectra of HL–Pb upon increasing concentration

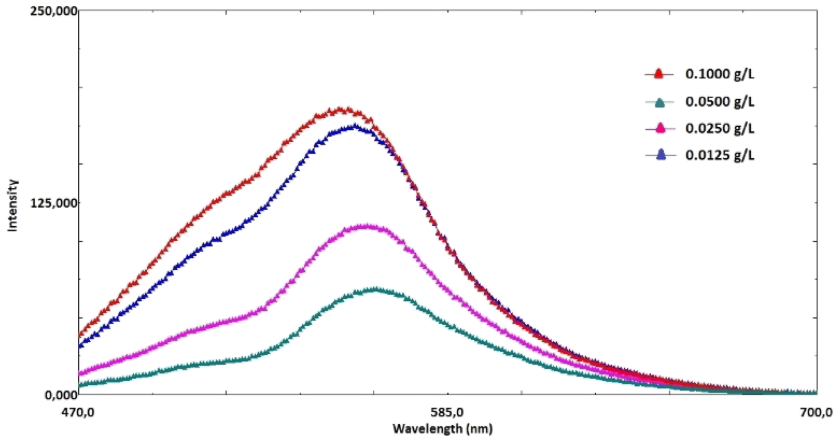

FIGURE 7 Florescence emission spectra of PL upon increasing concentration

kept constant as 1.00 mM and excited with 490 nm, the intensity of the HL complex with Pb^{2+}, Fe^{3+}, Ni^{2+}, Zn^{2+}, Mn^{2+}, Hg^{2+}, bare HL, and Ag^{+} metals were found to be 938, 326, 224, 150, 92, 58, 14, and 2 a.u., respectively, at 544 nm, which is the maximum emission wavelength. The fluorescence intensity of HL appears to increase 67 times over bare HL with the addition of Pb^{2+}, indicating that HL can be used as a potential fluorescence probe for Pb^{2+}. It can be suggested that Pb^{2+} possibly interact with the nitrogen atoms of the imine groups in the HL.[46] It appears that fluorescence emission gradually quenched due to increased Pb^{2+} concentration compared with measured fluorescence emissions depending on different Pb^{2+} concentrations (Figure 6). Although HL has no fluorescence feature, it is seen in the fluorescence spectrum in Figure 7 that PL, the polymer synthesized from HL, emits 551 nm when excited with 460-nm light. It was also revealed that when the PL concentration is changed in the range of 0.0125–0.1000 g L^{-1}, the fluorescence intensity increases with increasing concentration.

4 | CONCLUSION

In this work, new [NiL], [ZnL], and [FeLCl] complexes with symmetric bisimine structure were obtained from the reaction of monoimine and metal ions in one step and characterized. Analytical and spectral data revealed that the rearranged monoimine ligand coordinated to the metal ion with two imine nitrogens and two proton-free phenolic oxygen atoms. Thus, Ni(II) and Zn(II) complexes of ONNO donor, square planar, and symmetrical bisimine were obtained. In square pyramidal [FeLCl] complex, while the ligand is attached to the metal by means of two nitrogen atoms and two phenolic oxygen atoms, the fifth coordination is completed with the chlorine molecule. The single-crystal structure of [FeLCl] was also approved by single-crystal X-ray analysis.

It was found that metal complexes have higher thermal stability than HL and PL, due to metal–oxygen and metal–nitrogen coordination bonds. Calculated E_g' values according to the CV analysis results show us that the optical properties of HL, [FeLCl], [NiL], and [ZnL] are close to each other, but [NiL] has slightly lower E_g' values. The solid-state electrical conductivity measurements of the iodine doped states of the synthesized compounds showed that theirs are on the semiconductor level. PL has approximately 35 times higher electrical conductivity than the others. Although HL has no fluorescence property, it was found that the PL shows fluorescence property. In addition, fluorescence measurements revealed that the complexes formed by HL in solution with various metal ions exhibit fluorescence properties and can even be used as a fluorescent probe for Pb^{2+}. The method could be developed for Pb^{2+} determination.

ACKNOWLEDGMENT

This work was supported by the Scientific Research Projects Coordination Unit of Istanbul University-Cerrahpaşa (Project Number FYL-2016-20292).

AUTHOR CONTRIBUTIONS

Eylem Dilmen Portakal: Funding acquisition; investigation; visualization. **Yeliz Kaya:** Formal analysis; methodology; visualization. **Emire Demirayak:** Data curation; investigation; visualization. **Elif Karacan Yeldir:** Data curation; investigation; visualization. **Ayşe Erçağ:** Conceptualization; data curation; formal analysis; funding acquisition; investigation; methodology; project administration; supervision. **İsmet Kaya:** Data curation; formal analysis; investigation; supervision; visualization.

CONFLICT OF INTEREST

The authors declare no conflict of interest.

DATA AVAILABILITY STATEMENT

The data that support the findings of this study are available from the corresponding author upon reasonable request.

ORCID

Eylem Dilmen Portakal https://orcid.org/0000-0003-3523-4889
Yeliz Kaya https://orcid.org/0000-0001-5606-8088
Emire Demirayak https://orcid.org/0000-0003-1108-218X
Elif Karacan Yeldir https://orcid.org/0000-0001-8638-1198
Ayşe Erçağ https://orcid.org/0000-0003-0578-5698
İsmet Kaya https://orcid.org/0000-0002-9813-2962

REFERENCES

[1] K. Maher, *Asian J. Chem.* **2018**, *30*, 1171.
[2] Y. W. Liu, C. H. Chen, A. T. Wu, *Analyst* **2012**, *137*, 5201.
[3] A. K. Das, S. Goswami, *Sens. Actuators B* **2017**, *245*, 1062.
[4] I. Sheikhshoaie, N. Lotfi, J. Sieler, H. Krautscheid, M. Khaleghi, *Transition Met. Chem.* **2018**, *43*, 555.
[5] Y. Matsushita, I.-C. Jang, T. Imai, K. Fukushima, J.-M. Lee, H.-R. Park, S.-C. Lee, *J. Wood Sci.* **2011**, *57*, 161.
[6] C. Sun, X. Miao, L. Zhang, W. Li, Z. Chang, *Inorg. Chim. Acta* **2018**, *478*, 112.
[7] A. Ohshima, A. Momotake, T. Arai, *J. Photochem. Photobiol. A* **2004**, *162*, 473.
[8] N. Ahmad, E. H. Anouar, A. M. Tajuddin, K. Ramasamy, B. M. Yamin, H. Bahron, *PLoS One* **2020**, *15*, e0231147.
[9] W. Al Zoubi, Y. G. Ko, *Appl. Organomet. Chem.* **2017**, *31*, e3574.
[10] X. Lei, N. Chelamalla, *Polyhedron* **2013**, *49*, 244.
[11] E. S. A. El-Samanody, S. A. AbouEl-Enein, E. M. Emara, *Appl. Organomet. Chem.* **2018**, *32*, e4262.
[12] L. Zhang, P. P. Yang, L. F. Li, Y. Y. Hu, Y. Gao, J. Tao, *Appl. Organomet. Chem.* **2020**, *34*, e5331.
[13] P. Karuppasamy, D. Thiruppathi, J. Vijaya Sundar, V. Rajapandian, M. Ganesan, T. Rajendran, S. Rajagopal, N. Nagarajan, P. Rajendran, V. K. Sivasubramanian, *Arabian J. Sci. Eng.* **2015**, *40*, 2945.
[14] V. K. Sivasubramanian, M. Ganesan, S. Rajagopal, R. Ramaraj, *J. Org. Chem.* **2002**, *67*, 1506.
[15] D. Murtinho, Z. N. da Rocha, A. S. Pires, R. P. Jiménez, A. M. Abrantes, M. Laranjo, A. C. Mamede, J. E. Casalta-Lopes, M. F. Botelho, A. A. Pais, *Appl. Organomet. Chem.* **2015**, *29*, 425.
[16] M. Kongot, D. S. Reddy, V. Singh, R. Patel, N. K. Singhal, A. Kumar, *Appl. Organomet. Chem.* **2020**, *34*, e5327.
[17] J. M. Yates, J. S. Fell, J. A. Miranda, B. F. Gherman, *J. Electrochem. Soc.* **2013**, *160*, G3080.
[18] S. B. Bateni, K. R. England, A. T. Galatti, H. Kaur, V. A. Mendiola, A. R. Mitchell, M. H. Vu, B. F. Gherman, J. A. Miranda, *Beilstein J. Org. Chem.* **2009**, *5*, 1.
[19] R. Francke, R. D. Little, *Chem. Soc. Rev.* **2014**, *43*, 2492.
[20] S. M. Emam, S. A. AbouEl-Enein, E. M. Emara, *J. Therm. Anal. Calorim.* **2017**, *127*, 1611.
[21] A. W. Kleij, *Dalton Trans.* **2009**, 4635.
[22] G. Consiglio, I. P. Oliveri, S. Failla, S. Di Bella, *Molecules* **2019**, *24*, 1.
[23] A. Korkmaz, A. Cetin, E. Kaya, E. Erdoğan, *J. Polym. Res.* **2018**, *25*, 1.
[24] M. A. Hussein, M. A. Abdel-Rahman, A. M. Asiri, K. A. Alamry, K. I. Aly, *Des. Monomers Polym.* **2012**, *15*, 431.
[25] H. Karaer, İ. Kaya, H. Aydın, *Polimery* **2017**, *62*, 170.
[26] A. Erçağ, M. Şahin, A. Koca, E. Bozkurt, *J. Coord. Chem.* **2013**, *66*, 1635.
[27] M. Asadi, Z. Asadi, S. B. Sadi, L. Zarei, F. M. Baigi, Z. Amirghofran, *Spectrochim. Acta A Mol. Biomol. Spectrosc.* **2014**, *122*, 118.
[28] M. Asadi, H. Sepehrpour, K. Mohammadi, *J. Serb. Chem. Soc.* **2011**, *76*, 63.
[29] J. Cisterna, V. Artigas, M. Fuentealba, P. Hamon, C. Manzur, J.-R. Hamon, D. Carrillo, *Inorganics* **2018**, *6*, 1.
[30] M. A. Nasseri, K. Hemmat, A. Allahresani, *Appl. Organomet. Chem.* **2019**, *33*, e4743.
[31] G. M. Sheldrick, *Acta Crystallogr. Sect. A: Found. Crystallogr.* **2008**, *64*, 112.
[32] G. M. Sheldrick, *Acta Crystallogr. C Struct. Chem.* **2015**, *71*, 3.
[33] E. Tas, A. Kilic, M. Durgun, L. Kupecik, I. Yilmaz, S. Arslan, *Spectrochim. Acta A Mol. Biomol. Spectrosc.* **2010**, *75*, 811.
[34] H. A. R. Pramanik, P. C. Paul, P. Mondal, C. R. Bhattacharjee, *J. Mol. Struct.* **2015**, *1100*, 496.
[35] M. Asadi, M. S. Khah, *J. Iran. Chem. Soc.* **2010**, *7*, 875.
[36] M. A. Hadi, I. K. Kareem, *Res. J. in Adv. Sci.* **2020**, *1*, 54.
[37] D. Çakmak, S. Çakran, S. Yalçinkaya, C. Demetgül, *J. Electroanal. Chem.* **2018**, *808*, 65.
[38] H. Bahron, S. S. Khaidir, A. M. Tajuddin, K. Ramasamy, B. M. Yamin, *Polyhedron* **2019**, *161*, 84.
[39] A. M. Alosaimi, I. E. Mannoubi, S. A. Zabin, *Orient. J. Chem.* **2020**, *36*, 373.
[40] Y. X. Zhou, X. F. Zheng, D. Han, H. Y. Zhang, X. Q. Shen, C. Y. Niu, P. K. Chen, H. W. Hou, Y. Zhu, *Synth. React. Inorg. Met.-Org. Nano-Met. Chem* **2006**, *36*, 693.
[41] B. Kaya, O. Şahin, M. Bener, B. Ülküseven, *J. Mol. Struct.* **2018**, *1167*, 16.
[42] A. W. Addison, T. N. Rao, J. Reedijk, J. van Rijn, G. C. Verschoor, *J. Chem. Soc. Dalton Trans.* **1984**, 1349.
[43] İ. Kaya, A. Erçağ, S. Çulhaoğlu, *Inorg. Chim. Acta* **2020**, *508*, 119642.
[44] W. Liu, S.-H. Lee, S. Yang, S. Bian, L. Li, L. A. Samuelson, J. Kumar, S. K. Tripathy, *J. Macromol. Sci. Part A* **2001**, *38*, 1355.
[45] R. Cernini, X. Li, G. Spencer, A. Holmes, S. Moratti, R. Friend, *Synth. Met.* **1997**, *84*, 359.
[46] F. Kolcu, D. Erdener, İ. Kaya, *Inorg. Chim. Acta* **2020**, *509*, 119676.

SUPPORTING INFORMATION

Additional supporting information may be found online in the Supporting Information section at the end of this article.

How to cite this article: Dilmen Portakal E, Kaya Y, Demirayak E, Karacan Yeldir E, Erçağ A, Kaya İ. Synthesis, characterization, and investigation of some properties of the new symmetrical bisimine Ni(II), Zn(II), and Fe(III) complexes derived from the monoimine ligand. *Appl Organomet Chem*. 2021;35:e6265. https://doi.org/10.1002/aoc.6265